

Visualization and Decomposition of Through-focus images for Defect Detection via Phase-space tomography under Partially Coherent Illumination

Se Baek Oh, WIN division

A new method of analyzing and visualizing through-focus images is presented for potential sensitivity improvement and applications in defect detection and potentially optical review/classification. From through-focus intensity images the Wigner Distribution Function (WDF) and mutual intensity can be reconstructed, where partial coherence is rigorously modeled. Singular value decomposition (SVD) of mutual intensity further provides the amplitude and phase of individual coherent modes of light.

I. Introduction

This paper presents a new method of analyzing and visualizing through-focus images for defect detection and potentially optical defect review and classification. By taking advantages of multiple images collected over defocus, partial coherence is rigorously modeled and the WDF/mutual intensity are recovered.

Using coherent mode decomposition further allows not only easier comparison between reference and target images but also both amplitude and phase of each coherent mode, which can further improve sensitivity and enhance S/R.

The core idea and analysis flow are shown in Fig. 1.

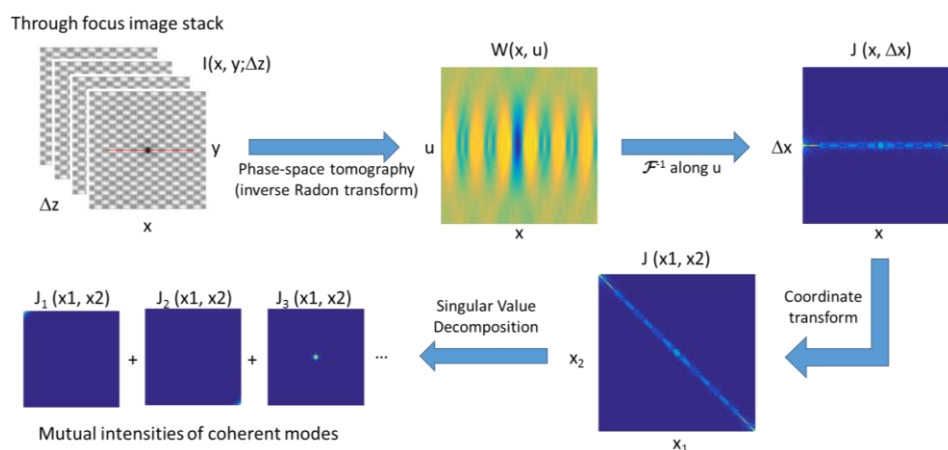


Fig. 1. Schematic of the data process: from through-focus image stack, the WDF can be reconstructed by phase-space tomography. Taking inverse Fourier transform along u (local spatial frequency) brings the WDF back to mutual intensity. Once mutual intensity is recovered, SVD (singular value decomposition) provides the mutual intensity of each coherent mode. All of the WDF, mutual intensity, and individual modes can be used for defect detection, review, and classification

A. Broadband plasma patterned wafer inspector as optical microscope under partially coherent light

The broadband plasma (BBP) wafer inspector is essentially an optical microscope; indeed it is a very complicated one with diffraction limited imaging performance and high magnification, wide spectral band and powerful light source, multiple imaging modes including bright field, dark field, and polarization, and super-fast post-image processing capability. As typical optical microscopes, BBP tools collect intensity imaged under partially coherent illumination. This implies that not only the phase of wave field is lost due to intensity only measurement, but also the phase of wave field is not well defined due to partial coherence. Nevertheless, phase of wave field, even if it is partially coherent, may have valuable information about defect, but currently BBP tools have focused on maximizing signals in intensity difference images.

In this paper, I present a new way of analyzing and visualizing through-focus images with the hope of recovering phase of partially coherent wave fields by using mathematical formulations developed for partial coherence – WDF, mutual intensity, and coherent mode decomposition. It has potential applications in (phase-sensitive) defect detection, and/or optical defect review and classification, or it may be able to improve S/N ratio or defect sensitivity.

In the following sections, the framework of the proposed method will be presented with an example from DSW. For simplicity, intensity images are assumed to be in 1D geometry such that the WDF and the mutual intensity become 2D quantities, which is easy to visualize and to use SVD instead of 4D WDF and mutual intensity.

B. Partial coherence formulation

In statistical optics [1], spatially partially coherent waves are represented by the (ensemble averaged) cross-correlation of the fields at two spatial points, $J(x_1, x_2) = \langle E(x_1)E^*(x_2) \rangle$, where J is called mutual intensity, E denotes the field of light, x_1 and x_2 are lateral spatial coordinates, $\langle \rangle$ is ensemble average, and $*$ denotes complex conjugate. If the field is

fully coherent, $J(x_1, x_2)$ has some values over entire x_1 - x_2 plane. If the field is fully incoherent, $J(x_1, x_2) = I(x_1)\delta(x_1 - x_2)$; correlation is zero when $x_1 \neq x_2$. Note that $J(x, x) = I(x)$ regardless of coherence state. Typically, measuring mutual intensity involves Michelson stellar interferometer [2] or shearing interferometers [3]; the magnitude and phase of mutual intensity can be obtained by the contrast change and phase of the interference fringes [4]. Using interferometers have obvious drawbacks; interferometric measurement is very sensitive to noise and environment. And also it is time-consuming to measure mutual intensity over wide (x_1, x_2) coverage and phase delay.

Phase-space tomography [5] uses only intensity measurement to reconstruct the WDF and subsequently back-calculates mutual intensity; hence it is much more straightforward and easier to implement than interferometric measurement.

II. Phase-space tomography: from through-focus intensity to mutual intensity

A. Wigner Distribution Function (WDF)

In phase-space tomography, from a series of intensity measurement over defocus, the WDF of the field is reconstructed by inverse Radon transform. Once the WDF is obtained, mutual intensity can be reconstructed easily.

Let me first introduce the WDF [6]. For a coherent field $E(x)$, the WDF is defined as

$$\mathcal{W}(x, u) = \int_{-\infty}^{\infty} E\left(x + \frac{x'}{2}\right) E^*\left(x - \frac{x'}{2}\right) e^{-j2\pi x' u} dx',$$

(Eq. 1)

where u is local spatial frequency. This definition can be extended to partially coherent wave because the quantity inside the integral in **Eq. 1** is essentially mutual intensity; hence the WDF can be also defined for partially coherent field as

$$\mathcal{W}(x, u) = \int_{-\infty}^{\infty} J(x, \Delta x) e^{-j2\pi(\Delta x)u} d(\Delta x).$$

(Eq. 2)

If we have 1D field $E(x)$, as it has both amplitude and phase, indeed we have 2D

information. As the WDF of 1D field is represented in 2D space ($x-u$), using the WDF is a useful way of visualizing the field, where both amplitude and phase are encoded and represented, even if the field is partially coherent.

The WDF has many interesting and useful properties [7] and a few notable ones are as follows: 1) WDF is always real, 2) the projection of the WDF along u is intensity, and 3) Fresnel propagation (under paraxial approximation) is represented as a simple x-shear transform ($\mathcal{W}_z(x, u) = \mathcal{W}(x, u - \lambda zu)$, where λ is the wavelength of the field and z is the propagation distance).

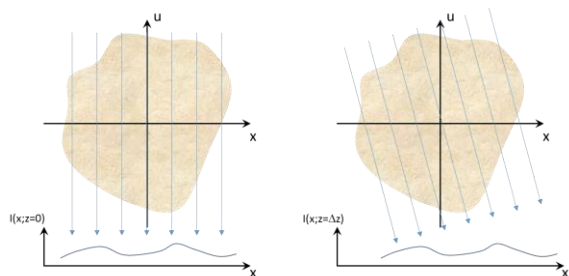


Fig. 2. Intensity is a projection of the WDF along u . As defocus shears the WDF, intensity at a defocused plan corresponds to a projection along sheared angle. In the paraxial regime, the x-shear can be approximated as rotation.

The last two properties constitute the basis of phase-space tomography: as the projection of the WDF at a certain angle corresponds to intensity measurement over defocus, where x-shear transform can be approximated as rotation in the paraxial region with a small defocus, getting a series of intensity measurement can fill the WDF in its Fourier domain (this is called Ambiguity function). Once we have enough "slices" in the Fourier domain, by using inverse Radon transform (Filtered back-projection), we can recover the WDF.

For easier understanding, let's think about the analogy with conventional x-ray CT, where 2D bone density is retrieved from a series of 1D projections: The bone density map corresponds to the WDF, and taking the projection at one angle is equivalent to get the intensity measurement at a certain defocused plane. As a series of x-ray projection is taken over a range of projection angle in x-ray CT, a series of intensity are measured at a range of defocus distance in phase-space tomography. Once we get the

projections (i.e., intensity stack), then usual inverse Radon transform/filtered-back projection can be used to reconstruct the original bone density map (i.e., WDF) as shown in Fig. 3.

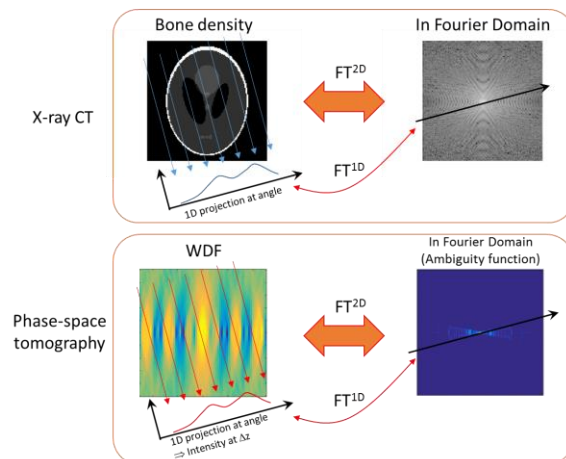


Fig. 3. Analogy between x-ray CT and phase-space tomography

As adjustable focus offset is limited in BBP tools, the reconstructed WDF from intensity measurements won't be perfect. To improve the accuracy, either more measurements are needed or some other priori or constraint can be used during the back-projection.

The WDF can be directly used for defect detection or review as clearly the difference between target and reference images may show up. As an example, the following pictures are taken from DSW.

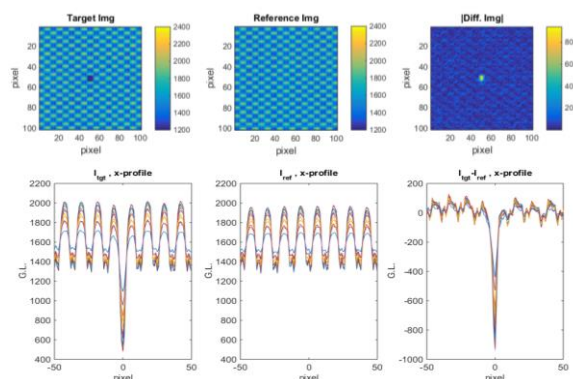


Fig. 4. Example images from DSW. Top row - 2D intensity images at best focus: reference (left), target (middle), and difference (right). Bottom row - overlaid 1D intensity profiles over 11 defocus distances: target (left), reference (middle), and difference (right). The maximum defocus distance is less than $\pm 300\text{nm}$.

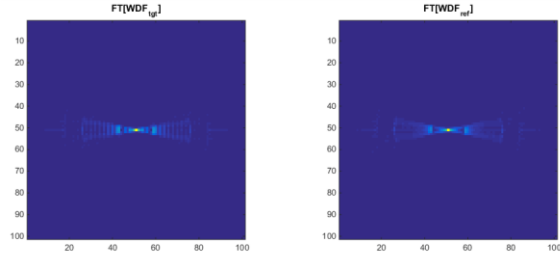


Fig. 5. Fourier domain representation of the WDF, where 1D intensity slices are filled with proper angles depending on the defocus: target (left) and reference (right). The inverse Radon transform is applied to these data to back-calculate the WDF.

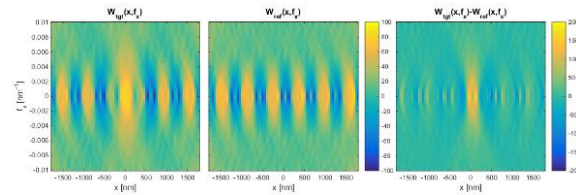


Fig. 6. Recovered WDF from target (left) and reference (middle) images. The difference between the target and reference WDFs is shown on the right. This contains the information how the difference signal behaves over defocus.

Although the WDF is real valued, it includes and visualizes phase information as its dimension gets doubled. Potentially, if we had phase defects, the WDF might be able to provide a signature of the phase defects, which is not shown up in intensity images.

B. WDF to mutual intensity

Once the WDF is obtained from intensity measurement, then mutual intensity can be calculated by the inverse Fourier transform along u ;

$$J(x, \Delta x) = \int_{-\infty}^{\infty} \mathcal{W}(x, u) e^{j2\pi(\Delta x)u} du. \quad (\text{Eq. 3})$$

Figure 6 shows the recovered mutual intensity in $(x, \Delta x)$ coordinates as well as (x_1, x_2) coordinates by using 45° rotation. These two steps are shown in Fig. 6. Note that mutual intensity is nearly concentrated near the diagonal, which implies that the light is close to incoherent (but not perfectly incoherent) as the

images are collected with BF.

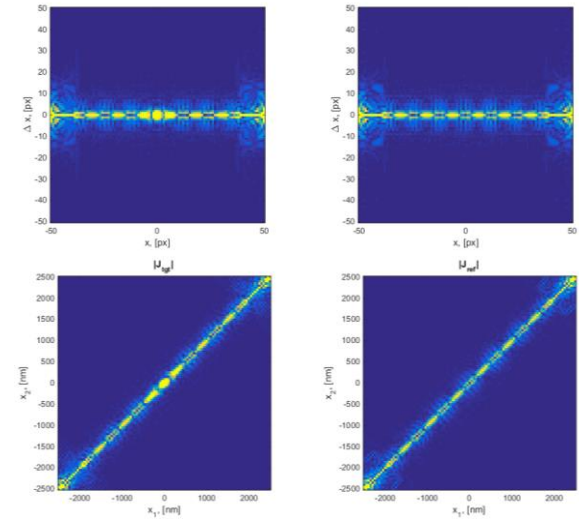


Fig. 7. Recovered mutual intensity in WDF in $(x-\Delta x)$ plane (top row) and (x_1-x_2) plane (bottom row). Left column is target and right column is reference, respectively.

C. Coherent mode decomposition

One of the reason why we want to convert the WDF into mutual intensity is to use “coherent mode decomposition” [8]. As partially coherent light can be considered as an average of multiple coherent wave, coherent mode decomposition, as the name suggests, decomposes the partially coherent light into individual coherent modes.

Numerically, as J is Hessian, simple SVD (Singular Value Decomposition) [9] can be used:

$$J = F \Sigma F^H \quad (\text{Eq. 3})$$

where Σ is a diagonal matrix consisting of the singular values σ_i , F is an orthogonal matrix consisting of individual coherent mode, and H is Hermitian operator. Note that this individual coherent mode is not necessarily the physical mode excited by a certain illumination as this is numerical decomposition.

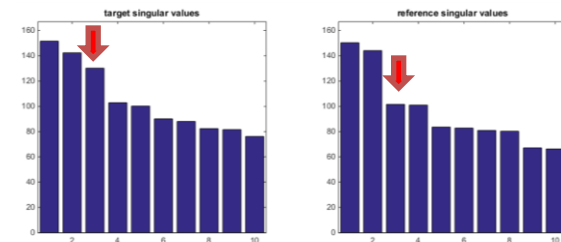


Fig. 8. First 10 singular values of the target and reference mutual intensities. Note that the third singular values are noticeably different.

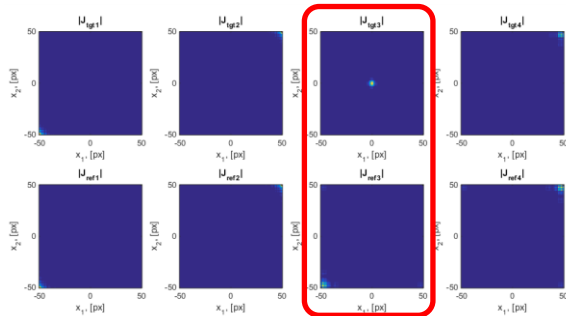


Fig. 9. First 4 coherent modes. Top row: target. Bottom row: reference. i th column corresponds to i th coherent mode. 3rd mode shows obvious difference.

Figure 8 shows the first 10 singular values, where the 3rd singular value is noticeably different. Figure 9 shows the mutual intensity of first 4 coherent modes. Again, the mutual intensity of the 3rd mode clearly shows the difference.

By looking at prominent modes we might be able to improve the S/N or defect fidelity.

III. Conclusion

This paper presents a new method of analyzing and visualizing through-focus images for defect detection and potentially optical defect review and classification. By taking advantages of multiple images collected over defocus, partial coherence is rigorously modeled and the WDF/mutual intensity are recovered. Using coherent mode decomposition further allows not only easier comparison between reference and target images but also both amplitude and phase of each coherent mode, which can further improve sensitivity and enhance S/R.

Acknowledgment

The author thanks Grace Chen for providing through-focus images and inspiration for looking at through focus images.

Bibliography

- [1] J. W. Goodman, *Statistical Optics*, New York: John Wiley & Sons, 1985.
- [2] A. A. Michelson, "On the application of interference methods to astronomical measurements," *The Astrophysical Journal*, vol. 51, pp. 257-262, 1920.
- [3] F. Roddier, "Interferometric imaging in optical astronomy," *Phys. Rep.*, vol. 170, pp. 97-166, 1988.
- [4] R. A. S. a. D. J. B. D. L. Marks, "Three-dimensional coherence imaging in the Fresnel domain," *Appl. Opt.*, vol. 38, no. 8, pp. 1332-1342, 1999.
- [5] J. L. S. B. O. a. G. B. L. Tian, "Experimental compressive phase space tomography," *Optics Express*, vol. 20, no. 8, pp. 8296-8308, 2012.
- [6] M. J. Bastiaan, "Wigner Distribution Function and Its Application to 1st-order Optics," *JOSA*, vol. 69, no. 12, pp. 1710-1716, 1979.
- [7] M. J. Bastiaans, "Application of the Wigner Distribution Function to Partially Coherent-light," *JOSA A*, vol. 3, no. 8, pp. 1227-1238, 1986.
- [8] M. B. a. E. Wolf, *Principles of Optics*, New York: Cambridge University Press, 1999.
- [9] Z. Zhang, *Analysis and synthesis of three-dimensional illumination using partial coherence*, Stanford University, 2011.